13

Airworthiness

The airworthiness of an aircraft is concerned with the standards of safety incorporated in all aspects of its construction. These range from structural strength to the provision of certain safeguards in the event of crash landings, and include design requirements relating to aerodynamics, performance and electrical and hydraulic systems. The selection of minimum standards of safety is largely the concern of 'national and international' airworthiness authorities who prepare handbooks of official requirements. The handbooks include operational requirements, minimum safety requirements, recommended practices and design data, etc.

In this chapter we shall concentrate on the structural aspects of airworthiness which depend chiefly on the strength and stiffness of the aircraft. Stiffness problems may be conveniently grouped under the heading *aeroelasticity* and are discussed in Section B6. Strength problems arise, as we have seen, from ground and air loads, and their magnitudes depend on the selection of manoeuvring and other conditions applicable to the operational requirements of a particular aircraft.

13.1 Factors of safety-flight envelope

The control of weight in aircraft design is of extreme importance. Increases in weight require stronger structures to support them, which in turn lead to further increases in weight and so on. Excesses of structural weight mean lesser amounts of payload, thereby affecting the economic viability of the aircraft. The aircraft designer is therefore constantly seeking to pare his aircraft's weight to the minimum compatible with safety. However, to ensure general minimum standards of strength and safety, airworthiness regulations lay down several factors which the primary structure of the aircraft must satisfy. These are the *limit load*, which is the maximum load that the aircraft is expected to experience in normal operation, the *proof load*, which is the product of the limit load and the *proof factor* (1.0–1.25), and the *ultimate load*, which is the product of the limit load and the *ultimate factor* (usually 1.5). The aircraft's structure must withstand the proof load without detrimental distortion and should not fail until the ultimate load has been achieved. The proof and ultimate factors may be regarded as factors of safety and provide for various contingencies and uncertainties which are discussed in greater detail in Section 13.2.

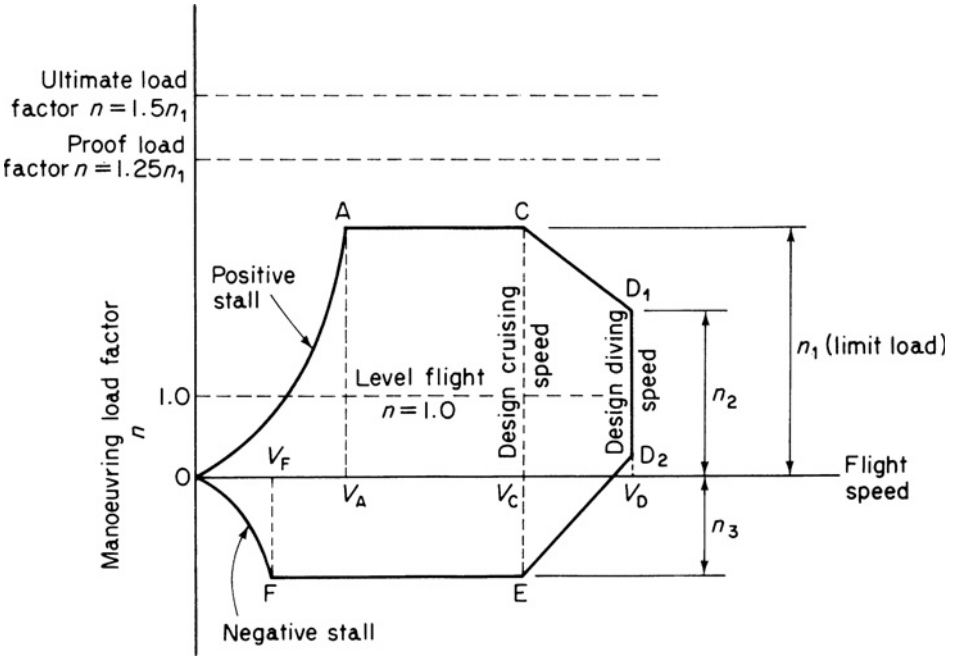

Fig. 13.1 Flight envelope

Table 13.1

	Category		
Load factor n	Normal	Semi-aerobatic	Aerobatic
n_1	$2.1 + 24\,000/(W + 10\,000)$	4.5	6.0
n_2	$0.75n_1$ but $n_2 \nless 2.0$	3.1	4.5
n_3	1.0	1.8	3.0

The basic strength and flight performance limits for a particular aircraft are selected by the airworthiness authorities and are contained in the *flight envelope* or *V–n* diagram shown in Fig. 13.1. The curves OA and OF correspond to the stalled condition of the aircraft and are obtained from the well-known aerodynamic relationship

$$\text{Lift} = nW = \tfrac{1}{2}\rho V^2 S C_{\text{L,max}}$$

Therefore, for speeds below V_A (positive wing incidence) and V_F (negative incidence) the maximum loads which can be applied to the aircraft are governed by $C_{\text{L,max}}$. As the speed increases it is possible to apply the positive and negative limit loads, corresponding to n_1 and n_3, without stalling the aircraft so that AC and FE represent maximum operational load factors for the aircraft. Above the design cruising speed V_C, the cut-off lines CD_1 and D_2E relieve the design cases to be covered since it is not expected that the limit loads will be applied at maximum speed. Values of n_1, n_2 and n_3 are specified by the airworthiness authorities for particular aircraft; typical load factors are shown in Table 13.1.

A particular flight envelope is applicable to one altitude only since $C_{L,max}$ is generally reduced with an increase of altitude, and the speed of sound decreases with altitude thereby reducing the critical Mach number and hence the design diving speed V_D. Flight envelopes are therefore drawn for a range of altitudes from sea level to the operational ceiling of the aircraft.

13.2 Load factor determination

Several problems require solution before values for the various load factors in the flight envelope can be determined. The limit load, for example, may be produced by a specified manoeuvre or by an encounter with a particularly severe gust (gust cases and the associated gust envelope are discussed in Section 14.4). Clearly some knowledge of possible gust conditions is required to determine the limiting case. Furthermore, the fixing of the proof and ultimate factors also depends upon the degree of uncertainty of design, variations in structural strength, structural deterioration, etc. We shall now investigate some of these problems to see their comparative influence on load factor values.

13.2.1 Limit load

An aircraft is subjected to a variety of loads during its operational life, the main classes of which are: manoeuvre loads, gust loads, undercarriage loads, cabin pressure loads, buffeting and induced vibrations. Of these, manoeuvre, undercarriage and cabin pressure loads are determined with reasonable simplicity since manoeuvre loads are controlled design cases, undercarriages are designed for given maximum descent rates and cabin pressures are specified. The remaining loads depend to a large extent on the atmospheric conditions encountered during flight. Estimates of the magnitudes of such loads are only possible therefore if in-flight data on these loads is available. It obviously requires a great number of hours of flying if the experimental data are to include possible extremes of atmospheric conditions. In practice, the amount of data required to establish the probable period of flight time before an aircraft encounters, say, a gust load of a given severity, is a great deal more than that available. It therefore becomes a problem in statistics to extrapolate the available data and calculate the probability of an aircraft being subjected to its proof or ultimate load during its operational life. The aim would be for a zero or negligible rate of occurrence of its ultimate load and an extremely low rate of occurrence of its proof load. Having decided on an ultimate load, then the limit load may be fixed as defined in Section 13.1 although the value of the ultimate factor includes, as we have already noted, allowances for uncertainties in design, variation in structural strength and structural deterioration.

13.2.2 Uncertainties in design and structural deterioration

Neither of these presents serious problems in modern aircraft construction and therefore do not require large factors of safety to minimize their effects. Modern methods of aircraft structural analysis are refined and, in any case, tests to determine actual failure

loads are carried out on representative full scale components to verify design estimates. The problem of structural deterioration due to corrosion and wear may be largely eliminated by close inspection during service and the application of suitable protective treatments.

13.2.3 Variation in structural strength

To minimize the effect of the variation in structural strength between two apparently identical components, strict controls are employed in the manufacture of materials and in the fabrication of the structure. Material control involves the observance of strict limits in chemical composition and close supervision of manufacturing methods such as machining, heat treatment, rolling, etc. In addition, the inspection of samples by visual, radiographic and other means, and the carrying out of strength tests on specimens, enable below limit batches to be isolated and rejected. Thus, if a sample of a batch of material falls below a specified minimum strength then the batch is rejected. This means of course that an actual structure always comprises materials with properties equal to or better than those assumed for design purposes, an added but unallowed for 'bonus' in considering factors of safety.

Similar precautions are applied to assembled structures with regard to dimension tolerances, quality of assembly, welding, etc. Again, visual and other inspection methods are employed and, in certain cases, strength tests are carried out on sample structures.

13.2.4 Fatigue

Although adequate precautions are taken to ensure that an aircraft's structure possesses sufficient strength to withstand the most severe expected gust or manoeuvre load, there still remains the problem of fatigue. Practically all components of the aircraft's structure are subjected to fluctuating loads which occur a great many times during the life of the aircraft. It has been known for many years that materials fail under fluctuating loads at much lower values of stress than their normal static failure stress. A graph of failure stress against number of repetitions of this stress has the typical form shown in Fig. 13.2. For some materials, such as mild steel, the curve (usually known as an *S–N* curve or diagram) is asymptotic to a certain minimum value, which means that the material has an actual infinite-life stress. Curves for other materials, for example aluminium and its alloys, do not always appear to have asymptotic values so that these materials may not possess an infinite-life stress. We shall discuss the implications of this a little later.

Prior to the mid-1940s little attention had been paid to fatigue considerations in the design of aircraft structures. It was felt that sufficient static strength would eliminate the possibility of fatigue failure. However, evidence began to accumulate that several aircraft crashes had been caused by fatigue failure. The seriousness of the situation was highlighted in the early 1950s by catastrophic fatigue failures of two Comet airliners. These were caused by the once-per-flight cabin pressurization cycle which produced circumferential and longitudinal stresses in the fuselage skin. Although these stresses were well below the allowable stresses for single cycle loading, stress concentrations occurred at the corners of the windows and around rivets which raised local stresses

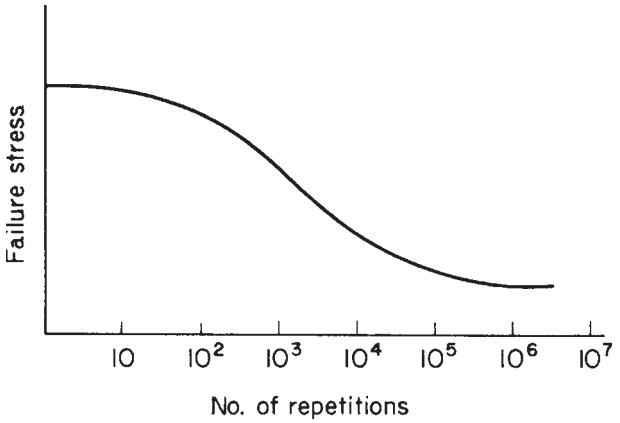

Fig. 13.2 Typical form of *S–N* diagram.

considerably above the general stress level. Repeated cycles of pressurization produced fatigue cracks which propagated disastrously, causing an explosion of the fuselage at high altitude.

Several factors contributed to the emergence of fatigue as a major factor in design. For example, aircraft speeds and sizes increased, calling for higher wing and other loadings. Consequently, the effect of turbulence was magnified and the magnitudes of the fluctuating loads became larger. In civil aviation, airliners had a greater utilization and a longer operational life. The new 'zinc-rich' alloys, used for their high static strength properties, did not show a proportional improvement in fatigue strength, exhibited high crack propagation rates and were extremely notch sensitive.

Despite the fact that the causes of fatigue were reasonably clear at that time its elimination as a threat to aircraft safety was a different matter. The fatigue problem has two major facets: the prediction of the fatigue strength of a structure and a knowledge of the loads causing fatigue. Information was lacking on both counts. The Royal Aircraft Establishment (RAE) and the aircraft industry therefore embarked on an extensive test programme to determine the behaviour of complete components, joints and other detail parts under fluctuating loads. These included fatigue testing by the RAE of some 50 Meteor 4 tailplanes at a range of temperatures, plus research, also by the RAE, into the fatigue behaviour of joints and connections. Further work was undertaken by some universities and by the industry itself into the effects of stress concentrations.

In conjunction with their fatigue strength testing, the RAE initiated research to develop a suitable instrument for counting and recording gust loads over long periods of time. Such an instrument was developed by J. Taylor in 1950 and was designed so that the response fell off rapidly above 10 Hz. Crossings of g thresholds from 0.2 to 1.8 g at 0.1 g intervals were recorded (note that steady level flight is 1 g flight) during experimental flying at the RAE on three different aircraft over 28 000 km, and the best techniques for extracting information from the data established. Civil airlines cooperated by carrying the instruments on their regular air services for a number of years. Eight different types of aircraft were equipped so that by 1961 records had been obtained for regions including Europe, the Atlantic, Africa, India and the Far East, representing 19 000 hours and 8 million km of flying.

Atmospheric turbulence and the cabin pressurization cycle are only two of the many fluctuating loads which cause fatigue damage in aircraft. On the ground the wing is supported on the undercarriage and experiences tensile stresses in its upper surfaces and compressive stresses in its lower surfaces. In flight these stresses are reversed as aerodynamic lift supports the wing. Also, the impact of landing and ground manoeuvring on imperfect surfaces cause stress fluctuations while, during landing and take-off, flaps are lowered and raised, producing additional load cycles in the flap support structure. Engine pylons are subjected to fatigue loading from thrust variations in take-off and landing and also to inertia loads produced by lateral gusts on the complete aircraft.

A more detailed investigation of fatigue and its associated problems is presented in Chapter 15 whilst a fuller discussion of airworthiness as applied to civil jet aircraft is presented in Ref. [1].

Reference

1 Jenkinson, L. R., Simpkin, P. and Rhodes, D., *Civil Jet Aircraft Design*, Arnold, London, 1999.

14

Airframe loads

In Chapter 12, we discussed in general terms the types of load to which aircraft are subjected during their operational life. We shall now examine in more detail the loads which are produced by various manoeuvres and the manner in which they are calculated.

14.1 Aircraft inertia loads

The maximum loads on the components of an aircraft's structure generally occur when the aircraft is undergoing some form of acceleration or deceleration, such as in landings, take-offs and manoeuvres within the flight and gust envelopes. Thus, before a structural component can be designed, the inertia loads corresponding to these accelerations and decelerations must be calculated. For these purposes we shall suppose that an aircraft is a rigid body and represent it by a rigid mass, m, as shown in Fig. 14.1. We shall also, at this stage, consider motion in the plane of the mass which would correspond to pitching of the aircraft without roll or yaw. We shall also suppose that the centre of gravity (CG) of the mass has coordinates $\bar{x}$, $\bar{y}$ referred to x and y axes having an arbitrary origin O; the mass is rotating about an axis through O perpendicular to the xy plane with a constant angular velocity ω.

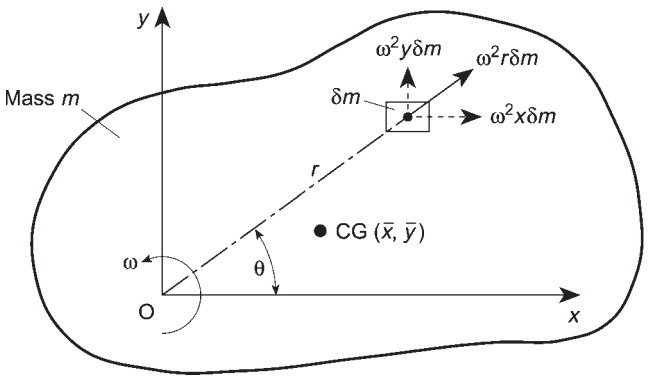

Fig. 14.1 Inertia forces on a rigid mass having a constant angular velocity.

The acceleration of any point, a distance r from O, is $\omega^2 r$ and is directed towards O. Thus, the inertia force acting on the element, δm, is $\omega^2 r \delta m$ in a direction opposite to the acceleration, as shown in Fig. 14.1. The components of this inertia force, parallel to the x and y axes, are $\omega^2 r \delta m \cos\theta$ and $\omega^2 r \delta m \, sin\, \theta$, respectively, or, in terms of x and y, $\omega^2 x \delta m$ and $\omega^2 y \delta m$. The resultant inertia forces, F_x and F_y, are then given by

$$F_x = \int \omega^2 x \, \mathrm{d}m = \omega^2 \int x \, \mathrm{d}m$$

$$F_y = \int \omega^2 y \, \mathrm{d}m = \omega^2 \int y \, \mathrm{d}m$$

in which we note that the angular velocity ω is constant and may therefore be taken outside the integral sign. In the above expressions $\int x \, \mathrm{d}m$ and $\int y \, \mathrm{d}m$ are the moments of the mass, m, about the y and x axes, respectively, so that

$$F_x = \omega^2 \bar{x} m \tag{14.1}$$

and

$$F_y = \omega^2 \bar{y} m \tag{14.2}$$

If the CG lies on the x axis, $\bar{y} = 0$ and $F_y = 0$. Similarly, if the CG lies on the y axis, $F_x = 0$. Clearly, if O coincides with the CG, $\bar{x} = \bar{y} = 0$ and $F_x = F_y = 0$.

Suppose now that the rigid body is subjected to an angular acceleration (or deceleration) α in addition to the constant angular velocity, ω, as shown in Fig. 14.2. An additional inertia force, $\alpha r \delta m$, acts on the element δm in a direction perpendicular to r and in the opposite sense to the angular acceleration. This inertia force has components $\alpha r \delta m \cos\theta$ and $\alpha r \delta m \sin\theta$, i.e. $\alpha x \delta m$ and $\alpha y \delta m$, in the y and x directions, respectively. Thus, the resultant inertia forces, F_x and F_y, are given by

$$F_x = \int \alpha y \, \mathrm{d}m = \alpha \int y \, \mathrm{d}m$$

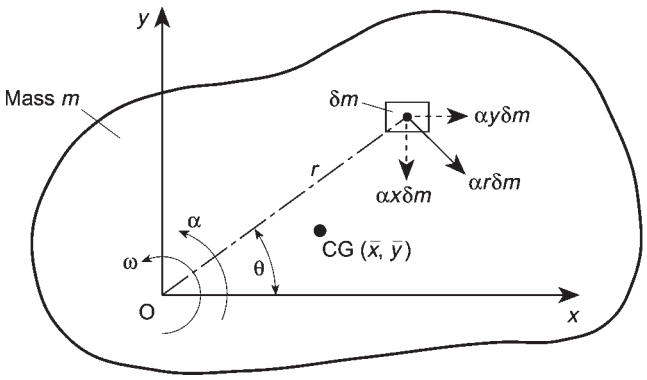

Fig. 14.2 Inertia forces on a rigid mass subjected to an angular acceleration.

and

$$F_y = -\int \alpha x \, \mathrm{d}m = -\alpha \int x \, \mathrm{d}m$$

for α in the direction shown. Then, as before

$$F_x = \alpha \bar{y} m \tag{14.3}$$

and

$$F_y = \alpha \bar{x} m \tag{14.4}$$

Also, if the CG lies on the x axis, $\bar{y} = 0$ and $F_x = 0$. Similarly, if the CG lies on the y axis, $\bar{x} = 0$ and $F_y = 0$.

The torque about the axis of rotation produced by the inertia force corresponding to the angular acceleration on the element δm is given by

$$\delta T_{\mathrm{O}} = \alpha r^2 \delta m$$

Thus, for the complete mass

$$T_{\mathrm{O}} = \int \alpha r^2 \, \mathrm{d}m = \alpha \int r^2 \, \mathrm{d}m$$

The integral term in this expression is the moment of inertia, I_{O}, of the mass about the axis of rotation. Thus

$$T_{\mathrm{O}} = \alpha I_{\mathrm{O}} \tag{14.5}$$

Equation (14.5) may be rewritten in terms of I_{CG}, the moment of inertia of the mass about an axis perpendicular to the plane of the mass through the CG. Hence, using the parallel axes theorem

$$I_{\mathrm{O}} = m(\bar{r})^2 + I_{\mathrm{CG}}$$

where $\bar{r}$ is the distance between O and the CG. Then

$$I_{\mathrm{O}} = m[(\bar{x})^2 + (\bar{y})^2] + I_{\mathrm{CG}}$$

and

$$T_{\mathrm{O}} = m[(\bar{x})^2 + (\bar{y})^2]\alpha + I_{\mathrm{CG}}\alpha \tag{14.6}$$

Example 14.1

An aircraft having a total weight of 45 kN lands on the deck of an aircraft carrier and is brought to rest by means of a cable engaged by an arrester hook, as shown in Fig. 14.3. If the deceleration induced by the cable is 3 g determine the tension, T, in the cable, the load on an undercarriage strut and the shear and axial loads in the fuselage at the section AA; the weight of the aircraft aft of AA is 4.5 kN. Calculate also the length of deck covered by the aircraft before it is brought to rest if the touch-down speed is 25 m/s.

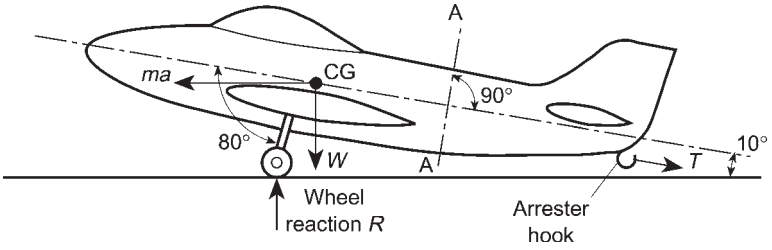

Fig. 14.3 Forces on the aircraft of Example 14.1.

The aircraft is subjected to a horizontal inertia force ma where m is the mass of the aircraft and a its deceleration. Thus, resolving forces horizontally

$$T\cos 10^\circ - ma = 0$$

i.e.

$$T\cos 10^\circ - \frac{45}{g}3\,g = 0$$

which gives

$$T = 137.1\,\text{kN}$$

Now resolving forces vertically

$$R - W - T\sin 10^\circ = 0$$

i.e.

$$R = 45 + 131.1\sin 10^\circ = 68.8\,\text{kN}$$

Assuming two undercarriage struts, the load in each strut will be $(R/2)/\cos 20^\circ = 36.6\,\text{kN}$.

Let N and S be the axial and shear loads at the section AA, as shown in Fig. 14.4. The inertia load acting at the CG of the fuselage aft of AA is $m_1 a$, where m_1 is the mass of the fuselage aft of AA. Then

$$m_1 a = \frac{4.5}{g}3\,g = 13.5\,\text{kN}$$

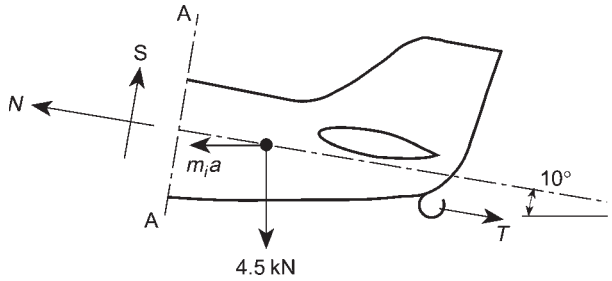

Fig. 14.4 Shear and axial loads at the section AA of the aircraft of Example 14.1.

Resolving forces parallel to the axis of the fuselage

$$N - T + m_1 a \cos 10^\circ - 4.5 \sin 10^\circ = 0$$

i.e.

$$N - 137.1 + 13.5 \cos 10^\circ - 4.5 \sin 10^\circ = 0$$

whence

$$N = 124.6\,\text{kN}$$

Now resolving forces perpendicular to the axis of the fuselage

$$S - m_1 a \sin 10^\circ - 4.5 \cos 10^\circ = 0$$

i.e.

$$S - 13.5 \sin 10^\circ - 4.5 \cos 10^\circ = 0$$

so that

$$S = 6.8\,\text{kN}$$

Note that, in addition to the axial load and shear load at the section AA, there will also be a bending moment.

Finally, from elementary dynamics

$$v^2 = v_0^2 + 2as$$

where v_0 is the touchdown speed, v the final speed (=0) and s the length of deck covered. Then

$$v_0^2 = -2as$$

i.e.

$$25^2 = -2(-3 \times 9.81)s$$

which gives

$$s = 10.6\,\text{m}$$

Example 14.2

An aircraft having a weight of 250 kN and a tricycle undercarriage lands at a vertical velocity of 3.7 m/s, such that the vertical and horizontal reactions on the main wheels are 1200 kN and 400 kN respectively; at this instant the nose wheel is 1.0 m from the ground, as shown in Fig. 14.5. If the moment of inertia of the aircraft about its CG is $5.65 \times 10^8\,\text{Ns}^2\,\text{mm}$ determine the inertia forces on the aircraft, the time taken for its vertical velocity to become zero and its angular velocity at this instant.

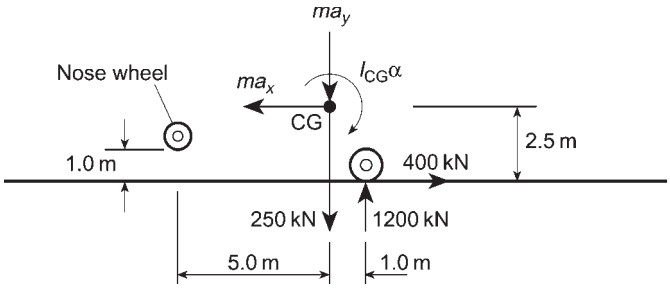

Fig. 14.5 Geometry of the aircraft of Example 14.2.

The horizontal and vertical inertia forces ma_x and ma_y act at the CG, as shown in Fig. 14.5, m is the mass of the aircraft and a_x and a_y its accelerations in the horizontal and vertical directions, respectively. Then, resolving forces horizontally

$$ma_x - 400 = 0$$

whence

$$ma_x = 400\,\text{kN}$$

Now resolving forces vertically

$$ma_y + 250 - 1200 = 0$$

which gives

$$ma_y = 950\,\text{kN}$$

Then

$$a_y = \frac{950}{m} = \frac{950}{250/g} = 3.8\,g \tag{i}$$

Now taking moments about the CG

$$I_{\text{CG}}\alpha - 1200 \times 1.0 - 400 \times 2.5 = 0 \tag{ii}$$

from which

$$I_{\text{CG}}\alpha = 2200\,\text{m kN}$$

Hence

$$\alpha = \frac{I_{\text{CG}}\alpha}{I_{\text{CG}}} = \frac{2200 \times 10^6}{5.65 \times 10^8} = 3.9\,\text{rad/s}^2 \tag{iii}$$

From Eq. (i), the aircraft has a vertical deceleration of 3.8 g from an initial vertical velocity of 3.7 m/s. Therefore, from elementary dynamics, the time, t, taken for the vertical velocity to become zero, is given by

$$v = v_0 + a_y t \tag{iv}$$

in which $v = 0$ and $v_0 = 3.7$ m/s. Hence

$$0 = 3.7 - 3.8 \times 9.81t$$

whence

$$t = 0.099\,\text{s}$$

In a similar manner to Eq. (iv) the angular velocity of the aircraft after 0.099 s is given by

$$\omega = \omega_0 + \alpha t$$

in which $\omega_0 = 0$ and $\alpha = 3.9\,\text{rad/s}^2$. Hence

$$\omega = 3.9 \times 0.099$$

i.e.

$$\omega = 0.39\,\text{rad/s}$$

14.2 Symmetric manoeuvre loads

We shall now consider the calculation of aircraft loads corresponding to the flight conditions specified by flight envelopes. There are, in fact, an infinite number of flight conditions within the boundary of the flight envelope although, structurally, those represented by the boundary are the most severe. Furthermore, it is usually found that the corners A, C, D_1, D_2, E and F (see Fig. 13.1) are more critical than points on the boundary between the corners so that, in practice, only the six conditions corresponding to these corner points need be investigated for each flight envelope.

In symmetric manoeuvres we consider the motion of the aircraft initiated by movement of the control surfaces in the plane of symmetry. Examples of such manoeuvres are loops, straight pull-outs and bunts, and the calculations involve the determination of lift, drag and tailplane loads at given flight speeds and altitudes. The effects of atmospheric turbulence and gusts are discussed in Section 14.4.

14.2.1 Level flight

Although steady level flight is not a manoeuvre in the strict sense of the word, it is a useful condition to investigate initially since it establishes points of load application and gives some idea of the equilibrium of an aircraft in the longitudinal plane. The loads acting on an aircraft in steady flight are shown in Fig. 14.6, with the following notation:

- L is the lift acting at the aerodynamic centre of the wing.
- D is the aircraft drag.
- M_0 is the aerodynamic pitching moment of the aircraft *less* its horizontal tail.
- P is the horizontal tail load acting at the aerodynamic centre of the tail, usually taken to be at approximately one-third of the tailplane chord.
- W is the aircraft weight acting at its CG.
- T is the engine thrust, assumed here to act parallel to the direction of flight in order to simplify calculation.

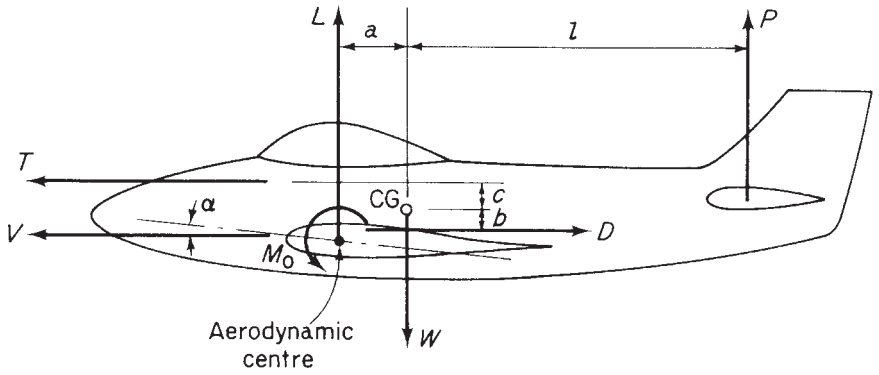

Fig. 14.6 Aircraft loads in level flight.

The loads are in static equilibrium since the aircraft is in a steady, unaccelerated, level flight condition. Thus for vertical equilibrium

$$L + P - W = 0 \tag{14.7}$$

for horizontal equilibrium

$$T - D = 0 \tag{14.8}$$

and taking moments about the aircraft's CG in the plane of symmetry

$$La - Db - Tc - M_0 - Pl = 0 \tag{14.9}$$

For a given aircraft weight, speed and altitude, Eqs (14.7)–(14.9) may be solved for the unknown lift, drag and tail loads. However, other parameters in these equations, such as M_0, depend upon the wing incidence α which in turn is a function of the required wing lift so that, in practice, a method of successive approximation is found to be the most convenient means of solution.

As a first approximation we assume that the tail load P is small compared with the wing lift L so that, from Eq. (14.7), $L \approx W$. From aerodynamic theory with the usual notation

$$L = \tfrac{1}{2}\rho V^2 S C_{\mathrm{L}}$$

Hence

$$\tfrac{1}{2}\rho V^2 S C_{\mathrm{L}} \approx W \tag{14.10}$$

Equation (14.10) gives the approximate lift coefficient C_{L} and thus (from $C_{\mathrm{L}}-\alpha$ curves established by wind tunnel tests) the wing incidence α. The drag load D follows (knowing V and α) and hence we obtain the required engine thrust T from Eq. (14.8). Also M_0, a, b, c and l may be calculated (again since V and α are known) and Eq. (14.9) solved for P. As a second approximation this value of P is substituted in Eq. (14.7) to obtain a more accurate value for L and the procedure is repeated. Usually three approximations are sufficient to produce reasonably accurate values.

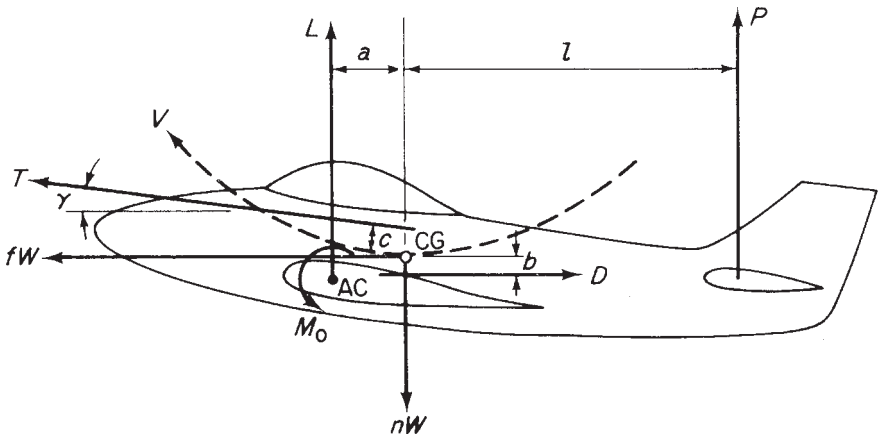

Fig. 14.7 Aircraft loads in a pull-out from a dive.

In most cases P, D and T are small compared with the lift and aircraft weight. Therefore, from Eq. (14.7) $L \approx W$ and substitution in Eq. (14.9) gives, neglecting D and T

$$P \approx W\frac{a}{l} - \frac{M_0}{l} \tag{14.11}$$

We see from Eq. (14.11) that if a is large then P will most likely be positive. In other words the tail load acts upwards when the CG of the aircraft is far aft. When a is small or negative, i.e., a forward CG, then P will probably be negative and act downwards.

14.2.2 General case of a symmetric manoeuvre

In a rapid pull-out from a dive a downward load is applied to the tailplane, causing the aircraft to pitch nose upwards. The downward load is achieved by a backward movement of the control column, thereby applying negative incidence to the elevators, or horizontal tail if the latter is all-moving. If the manoeuvre is carried out rapidly the forward speed of the aircraft remains practically constant so that increases in lift and drag result from the increase in wing incidence only. Since the lift is now greater than that required to balance the aircraft weight the aircraft experiences an upward acceleration normal to its flight path. This normal acceleration combined with the aircraft's speed in the dive results in the curved flight path shown in Fig. 14.7. As the drag load builds up with an increase of incidence the forward speed of the aircraft falls since the thrust is assumed to remain constant during the manoeuvre. It is usual, as we observed in the discussion of the flight envelope, to describe the manoeuvres of an aircraft in terms of a manoeuvring load factor n. For steady level flight $n = 1$, giving 1 g flight, although in fact the acceleration is zero. What is implied in this method of description is that the inertia force on the aircraft in the level flight condition is 1.0 times its weight. It follows that the vertical inertia force on an aircraft carrying out an ng manoeuvre is nW. We may therefore replace the dynamic conditions of the accelerated motion by an equivalent set of static conditions in which the applied loads are in equilibrium with

the inertia forces. Thus, in Fig. 14.7, n is the manoeuvre load factor while f is a similar factor giving the horizontal inertia force. Note that the actual normal acceleration in this particular case is $(n-1)g$.

For vertical equilibrium of the aircraft, we have, referring to Fig. 14.7 where the aircraft is shown at the lowest point of the pull-out

$$L + P + T\sin\gamma - nW = 0 \tag{14.12}$$

For horizontal equilibrium

$$T\cos\gamma + fW - D = 0 \tag{14.13}$$

and for pitching moment equilibrium about the aircraft's CG

$$La - Db - Tc - M_0 - Pl = 0 \tag{14.14}$$

Equation (14.14) contains no terms representing the effect of pitching acceleration of the aircraft; this is assumed to be negligible at this stage.

Again the method of successive approximation is found to be most convenient for the solution of Eqs (14.12)–(14.14). There is, however, a difference to the procedure described for the steady level flight case. The engine thrust T is no longer directly related to the drag D as the latter changes during the manoeuvre. Generally, the thrust is regarded as remaining constant and equal to the value appropriate to conditions before the manoeuvre began.

Example 14.3

The curves C_D, α and $C_{M,CG}$ for a light aircraft are shown in Fig. 14.8(a). The aircraft weight is 8000 N, its wing area 14.5 m^2 and its mean chord 1.35 m. Determine the lift, drag, tail load and forward inertia force for a symmetric manoeuvre corresponding to $n = 4.5$ and a speed of 60 m/s. Assume that engine-off conditions apply and that the air density is 1.223 kg/m^3. Figure 14.8(b) shows the relevant aircraft dimensions.

As a first approximation we neglect the tail load P. Therefore, from Eq. (14.12), since $T = 0$, we have

$$L \approx nW \tag{i}$$

Hence

$$C_L = \frac{L}{\frac{1}{2}\rho V^2 S} \approx \frac{4.5 \times 8000}{\frac{1}{2} \times 1.223 \times 60^2 \times 14.5} = 1.113$$

From Fig. 14.8(a), $\alpha = 13.75°$ and $C_{M,CG} = 0.075$. The tail arm l, from Fig. 14.8(b), is

$$l = 4.18\cos(\alpha - 2) + 0.31\sin(\alpha - 2) \tag{ii}$$

Substituting the above value of α gives $l = 4.123$ m. In Eq. (14.14) the terms $La - Db - M_0$ are equivalent to the aircraft pitching moment M_{CG} about its CG. Eq. (14.14) may therefore be written

$$M_{CG} - Pl = 0$$

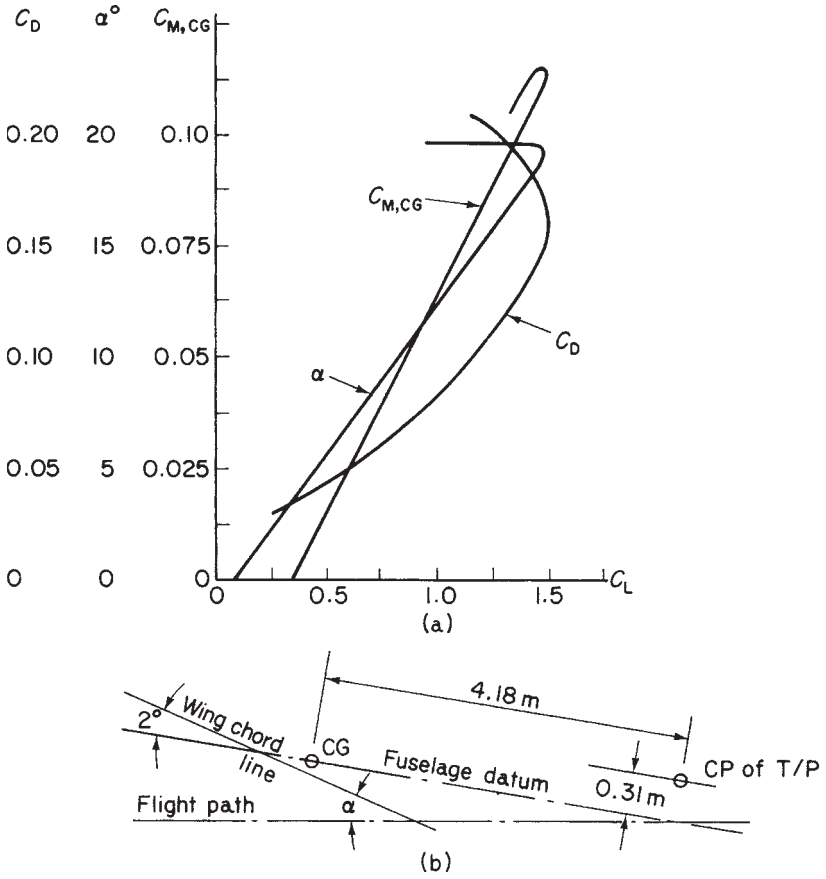

Fig. 14.8 (a) C_D, α, $C_{M,CG} - C_L$ curves for Example 14.3; (b) geometry of Example 14.3.

or

$$Pl = \tfrac{1}{2}\rho V^2 ScC_{M,CG} \qquad \text{(iii)}$$

where $c =$ wing mean chord. Substituting P from Eq. (iii) into Eq. (14.12) we have

$$L + \frac{\tfrac{1}{2}\rho V^2 ScC_{M,CG}}{l} = nW$$

or dividing through by $\tfrac{1}{2}\rho V^2 S$

$$C_L + \frac{c}{l}C_{M,CG} = \frac{nW}{\tfrac{1}{2}\rho V^2 S} \qquad \text{(iv)}$$

We now obtain a more accurate value for C_L from Eq. (iv)

$$C_L = 1.113 - \frac{1.35}{4.123} \times 0.075 = 1.088$$

giving $\alpha = 13.3°$ and $C_{M,CG} = 0.073$.

Substituting this value of α into Eq. (ii) gives a second approximation for l, namely $l = 4.161$ m.

Equation (iv) now gives a third approximation for C_L, i.e. $C_L = 1.099$. Since the three calculated values of C_L are all extremely close further approximations will not give values of C_L very much different to those above. Therefore, we shall take $C_L = 1.099$. From Fig. 14.8(a) $C_D = 0.0875$.

The values of lift, tail load, drag and forward inertia force then follow:

$$\text{Lift } L = \tfrac{1}{2}\rho V^2 S C_L = \tfrac{1}{2} \times 1.223 \times 60^2 \times 14.5 \times 1.099 = 35\,000 \text{ N}$$

$$\text{Tail load } P = nW - L = 4.5 \times 8000 - 35\,000 = 1000 \text{ N}$$

$$\text{Drag } D = \tfrac{1}{2}\rho V^2 S C_D = \tfrac{1}{2} \times 1.223 \times 60^2 \times 14.5 \times 0.0875 = 2790 \text{ N}$$

$$\text{Forward inertia force } fW = D \text{ (From Eq. (14.13))} = 2790 \text{ N}$$

14.3 Normal accelerations associated with various types of manoeuvre

In Section 14.2 we determined aircraft loads corresponding to a given manoeuvre load factor n. Clearly it is necessary to relate this load factor to given types of manoeuvre. Two cases arise: the first involving a steady pull-out from a dive and the second, a correctly banked turn. Although the latter is not a symmetric manoeuvre in the strict sense of the word, it gives rise to normal accelerations in the plane of symmetry and is therefore included.

14.3.1 Steady pull-out

Let us suppose that the aircraft has just begun its pull-out from a dive so that it is describing a curved flight path but is not yet at its lowest point. The loads acting on the aircraft at this stage of the manoeuvre are shown in Fig. 14.9, where R is the radius of curvature of the flight path. In this case the lift vector must equilibrate the normal (to the flight path) component of the aircraft weight and provide the force producing the centripetal acceleration V^2/R of the aircraft towards the centre of curvature of the flight path. Thus

$$L = \frac{WV^2}{gR} + W\cos\theta$$

or, since $L = nW$ (see Section 14.2)

$$n = \frac{V^2}{gR} + \cos\theta \tag{14.15}$$

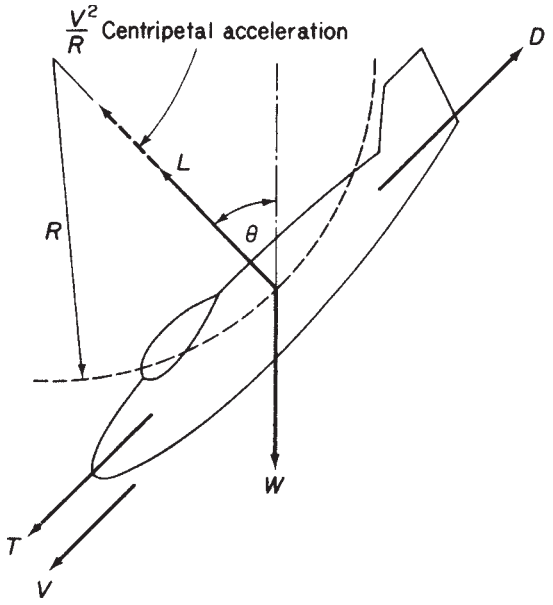

Fig. 14.9 Aircraft loads and acceleration during a steady pull-out.

At the lowest point of the pull-out, $\theta = 0$, and

$$n = \frac{V^2}{gR} + 1 \tag{14.16}$$

We see from either Eq. (14.15) or Eq. (14.16) that the smaller the radius of the flight path, that is the more severe the pull-out, the greater the value of n. It is quite possible therefore for a severe pull-out to overstress the aircraft by subjecting it to loads which lie outside the flight envelope and which may even exceed the proof or ultimate loads. In practice, the control surface movement may be limited by stops incorporated in the control circuit. These stops usually operate only above a certain speed giving the aircraft adequate manoeuvrability at lower speeds. For hydraulically operated controls 'artificial feel' is built in to the system whereby the stick force increases progressively as the speed increases; a necessary precaution in this type of system since the pilot is merely opening and closing valves in the control circuit and therefore receives no direct physical indication of control surface forces.

Alternatively, at low speeds, a severe pull-out or pull-up may stall the aircraft. Again safety precautions are usually incorporated in the form of stall warning devices since, for modern high speed aircraft, a stall can be disastrous, particularly at low altitude.

14.3.2 Correctly banked turn

In this manoeuvre the aircraft flies in a horizontal turn with no sideslip at constant speed. If the radius of the turn is R and the angle of bank ϕ, then the forces acting on

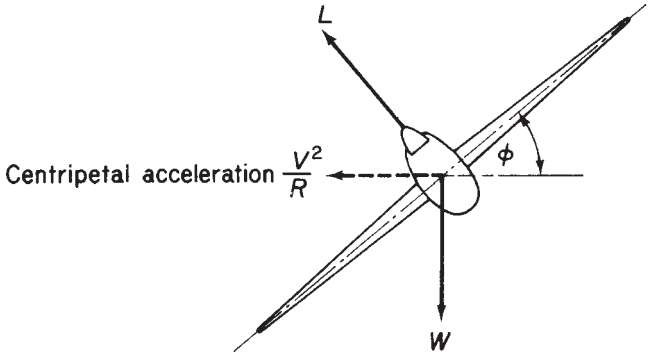

Fig. 14.10 Correctly banked turn.

the aircraft are those shown in Fig. 14.10. The horizontal component of the lift vector in this case provides the force necessary to produce the centripetal acceleration of the aircraft towards the centre of the turn. Then

$$L \sin \phi = \frac{WV^2}{gR} \tag{14.17}$$

and for vertical equilibrium

$$L \cos \phi = W \tag{14.18}$$

or

$$L = W \sec \phi \tag{14.19}$$

From Eq. (14.19) we see that the load factor n in the turn is given by

$$n = \sec \phi \tag{14.20}$$

Also, dividing Eq. (14.17) by Eq. (14.18)

$$\tan \phi = \frac{V^2}{gR} \tag{14.21}$$

Examination of Eq. (14.21) reveals that the tighter the turn the greater the angle of bank required to maintain horizontal flight. Furthermore, we see from Eq. (14.20) that an increase in bank angle results in an increased load factor. Aerodynamic theory shows that for a limiting value of n the minimum time taken to turn through a given angle at a given value of engine thrust occurs when the lift coefficient C_L is a maximum; that is, with the aircraft on the point of stalling.

14.4 Gust loads

In Section 14.2 we considered aircraft loads resulting from prescribed manoeuvres in the longitudinal plane of symmetry. Other types of in-flight load are caused by

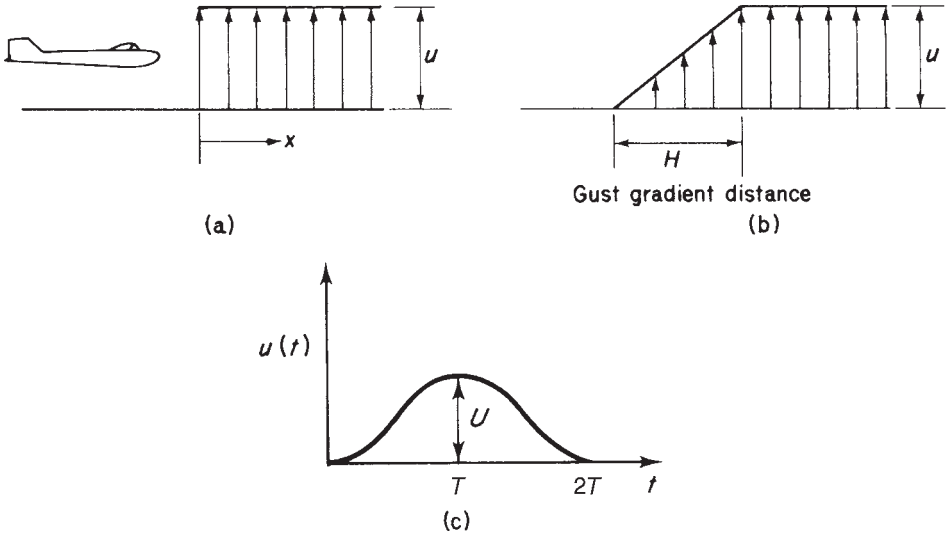

Fig. 14.11 (a) Sharp-edged gust; (b) graded gust; (c) 1 — cosine gust.

air turbulence. The movements of the air in turbulence are generally known as gusts and produce changes in wing incidence, thereby subjecting the aircraft to sudden or gradual increases or decreases in lift from which normal accelerations result. These may be critical for large, high speed aircraft and may possibly cause higher loads than control initiated manoeuvres.

At the present time two approaches are employed in gust analysis. One method, which has been in use for a considerable number of years, determines the aircraft response and loads due to a single or 'discrete' gust of a given profile. This profile is defined as a distribution of vertical gust velocity over a given finite length or given period of time. Examples of these profiles are shown in Fig. 14.11.

Early airworthiness requirements specified an instantaneous application of gust velocity u, resulting in the 'sharp-edged' gust of Fig. 14.11(a). Calculations of normal acceleration and aircraft response were based on the assumptions that the aircraft's flight is undisturbed while the aircraft passes from still air into the moving air of the gust and during the time taken for the gust loads to build up; that the aerodynamic forces on the aircraft are determined by the instantaneous incidence of the particular lifting surface and finally that the aircraft's structure is rigid. The second assumption here relating the aerodynamic force on a lifting surface to its instantaneous incidence neglects the fact that in a disturbance such as a gust there is a gradual growth of circulation and hence of lift to a steady state value (Wagner effect). This in general leads to an overestimation of the upward acceleration of an aircraft and therefore of gust loads.

The 'sharp-edged' gust was replaced when it was realized that the gust velocity built up to a maximum over a period of time. Airworthiness requirements were modified on the assumption that the gust velocity increased linearly to a maximum value over a specified gust gradient distance H. Hence the 'graded' gust of Fig. 14.11(b). In the UK, H is taken as 30.5 m. Since, as far as the aircraft is concerned, the gust velocity builds up to a maximum over a period of time it is no longer allowable to ignore the change of

flight path as the aircraft enters the gust. By the time the gust has attained its maximum value the aircraft has developed a vertical component of velocity and, in addition, may be pitching depending on its longitudinal stability characteristics. The effect of the former is to reduce the severity of the gust while the latter may either increase or decrease the loads involved. To evaluate the corresponding gust loads the designer may either calculate the complete motion of the aircraft during the disturbance and hence obtain the gust loads, or replace the 'graded' gust by an equivalent 'sharp-edged' gust producing approximately the same effect. We shall discuss the latter procedure in greater detail later.

The calculation of the complete response of the aircraft to a 'graded' gust may be obtained from its response to a 'sharp-edged' or 'step' gust, by treating the former as comprising a large number of small 'steps' and superimposing the responses to each of these. Such a process is known as convolution or Duhamel integration. This treatment is desirable for large or unorthodox aircraft where aeroelastic (structural flexibility) effects on gust loads may be appreciable or unknown. In such cases the assumption of a rigid aircraft may lead to an underestimation of gust loads. The equations of motion are therefore modified to allow for aeroelastic in addition to aerodynamic effects. For small and medium-sized aircraft having orthodox aerodynamic features the equivalent 'sharp-edged' gust procedure is satisfactory.

While the 'graded' or 'ramp' gust is used as a basis for gust load calculations, other shapes of gust profile are in current use. Typical of these is the '1 − cosine' gust of Fig. 14.11(c), where the gust velocity u is given by $u(t) = (U/2)[1 - \cos(\pi t/T)]$. Again the aircraft response is determined by superimposing the responses to each of a large number of small steps.

Although the 'discrete' gust approach still finds widespread use in the calculation of gust loads, alternative methods based on *power spectral* analysis are being investigated. The advantage of the power spectral technique lies in its freedom from arbitrary assumptions of gust shapes and sizes. It is assumed that gust velocity is a random variable which may be regarded for analysis as consisting of a large number of sinusoidal components whose amplitudes vary with frequency. The *power spectrum* of such a function is then defined as the distribution of energy over the frequency range. This may then be related to gust velocity. To establish appropriate amplitude and frequency distributions for a particular random gust profile requires a large amount of experimental data. The collection of such data has been previously referred to in Section 13.2.

Calculations of the complete response of an aircraft and detailed assessments of the 'discrete' gust and power spectral methods of analysis are outside the scope of this book. More information may be found in Refs [1–4] at the end of the chapter. Our present analysis is confined to the 'discrete' gust approach, in which we consider the 'sharp-edged' gust and the equivalent 'sharp-edged' gust derived from the 'graded' gust.

14.4.1 'Sharp-edged' gust

The simplifying assumptions introduced in the determination of gust loads resulting from the 'sharp-edged' gust, have been discussed in the earlier part of this section.

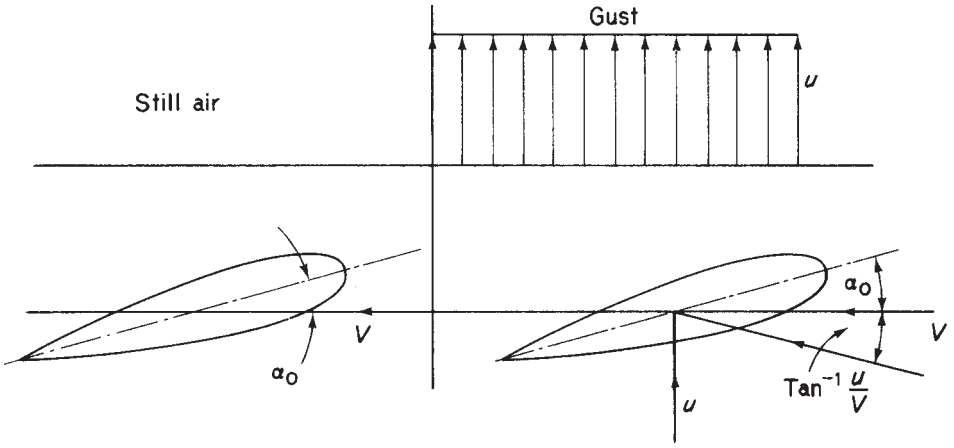

Fig. 14.12 Increase in wing incidence due to a sharp-edged gust.

In Fig. 14.12 the aircraft is flying at a speed V with wing incidence α_0 in still air. After entering the gust of upward velocity u, the incidence increases by an amount $\tan^{-1}u/V$, or since u is usually small compared with V, u/V. This is accompanied by an increase in aircraft speed from V to $(V^2+u^2)^{\frac{1}{2}}$, but again this increase is neglected since u is small. The increase in wing lift ΔL is then given by

$$\Delta L = \tfrac{1}{2}\rho V^2 S \frac{\partial C_\mathrm{L}}{\partial \alpha}\frac{u}{V} = \frac{1}{2}\rho V S \frac{\partial C_\mathrm{L}}{\partial \alpha}u \tag{14.22}$$

where $\partial C_\mathrm{L}/\partial\alpha$ is the wing lift–curve slope. Neglecting the change of lift on the tailplane as a first approximation, the gust load factor Δn produced by this change of lift is

$$\Delta n = \frac{\frac{1}{2}\rho V S(\partial C_\mathrm{L}/\partial\alpha)u}{W} \tag{14.23}$$

where W is the aircraft weight. Expressing Eq. (14.23) in terms of the wing loading, $w = W/S$, we have

$$\Delta n = \frac{\frac{1}{2}\rho V(\partial C_\mathrm{L}/\partial\alpha)u}{w} \tag{14.24}$$

This increment in gust load factor is additional to the steady level flight value $n = 1$. Therefore, as a result of the gust, the total gust load factor is

$$n = 1 + \frac{\frac{1}{2}\rho V(\partial C_\mathrm{L}/\partial\alpha)u}{w} \tag{14.25}$$

Similarly, for a downgust

$$n = 1 - \frac{\frac{1}{2}\rho V(\partial C_\mathrm{L}/\partial\alpha)u}{w} \tag{14.26}$$

If flight conditions are expressed in terms of equivalent sea-level conditions then V becomes the equivalent airspeed (EAS), V_E, u becomes u_E and the air density ρ is replaced by the sea-level value ρ_0. Equations (14.25) and (14.26) are written

$$n = 1 + \frac{\frac{1}{2}\rho_0 V_E(\partial C_L/\partial\alpha)u_E}{w} \tag{14.27}$$

and

$$n = 1 - \frac{\frac{1}{2}\rho_0 V_E(\partial C_L/\partial\alpha)u_E}{w} \tag{14.28}$$

We observe from Eqs (14.25)–(14.28) that the gust load factor is directly proportional to aircraft speed but inversely proportional to wing loading. It follows that high speed aircraft with low or moderate wing loadings are most likely to be affected by gust loads.

The contribution to normal acceleration of the change in tail load produced by the gust may be calculated using the same assumptions as before. However, the change in tailplane incidence is not equal to the change in wing incidence due to downwash effects at the tail. Thus if ΔP is the increase (or decrease) in tailplane load, then

$$\Delta P = \tfrac{1}{2}\rho_0 V_E^2 S_T \Delta C_{L,T} \tag{14.29}$$

where S_T is the tailplane area and $\Delta C_{L,T}$ the increment of tailplane lift coefficient given by

$$\Delta C_{L,T} = \frac{\partial C_{L,T}}{\partial\alpha}\frac{u_E}{V_E} \tag{14.30}$$

in which $\partial C_{L,T}/\partial\alpha$ is the rate of change of tailplane lift coefficient with wing incidence. From aerodynamic theory

$$\frac{\partial C_{L,T}}{\partial\alpha} = \frac{\partial C_{L,T}}{\partial\alpha_T}\left(1 - \frac{\partial\varepsilon}{\partial\alpha}\right)$$

where $\partial C_{L,T}/\partial\alpha_T$ is the rate of change of $C_{L,T}$ with tailplane incidence and $\partial\varepsilon/\partial\alpha$ the rate of change of downwash angle with wing incidence. Substituting for $\Delta C_{L,T}$ from Eq. (14.30) into Eq. (14.29), we have

$$\Delta P = \tfrac{1}{2}\rho_0 V_E S_T \frac{\partial C_{L,T}}{\partial\alpha} u_E \tag{14.31}$$

For positive increments of wing lift and tailplane load

$$\Delta nW = \Delta L + \Delta P$$

or, from Eqs (14.27) and (14.31)

$$\Delta n = \frac{\frac{1}{2}\rho_0 V_E(\partial C_L/\partial\alpha)u_E}{w}\left(1 + \frac{S_T}{S}\frac{\partial C_{L,T}/\partial\alpha}{\partial C_L/\partial\alpha}\right) \tag{14.32}$$

14.4.2 The 'graded' gust

The 'graded' gust of Fig. 14.11(b) may be converted to an equivalent 'sharp-edged' gust by multiplying the maximum velocity in the gust by a *gust alleviation factor*, F. Equation (14.27) then becomes

$$n = 1 + \frac{\frac{1}{2}\rho_0 V_E (\partial C_L/\partial\alpha) F u_E}{w} \tag{14.33}$$

Similar modifications are carried out on Eqs (14.25), (14.26), (14.28) and (14.32). The gust alleviation factor allows for some of the dynamic properties of the aircraft, including unsteady lift, and has been calculated taking into account the heaving motion (i.e. the up and down motion with zero rate of pitch) of the aircraft only.[5]

Horizontal gusts cause lateral loads on the vertical tail or fin. Their magnitudes may be calculated in an identical manner to those above, except that areas and values of lift curve slope are referred to the vertical tail. Also, the gust alleviation factor in the 'graded' gust case becomes F_1 and includes allowances for the aerodynamic yawing moment produced by the gust and the yawing inertia of the aircraft.

14.4.3 Gust envelope

Airworthiness requirements usually specify that gust loads shall be calculated at certain combinations of gust and flight speed. The equations for gust load factor in the above analysis show that n is proportional to aircraft speed for a given gust velocity. Therefore, we may plot a gust envelope similar to the flight envelope of Fig. 13.1, as shown in Fig. 14.13. The gust speeds $\pm U_1$, $\pm U_2$ and $\pm U_3$ are high, medium and low velocity gusts, respectively. Cut-offs occur at points where the lines corresponding to each gust

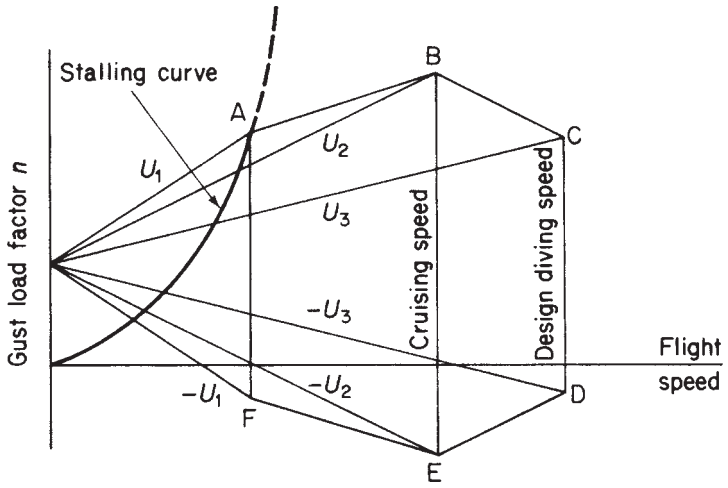

Fig. 14.13 Typical gust envelope.

velocity meet specific aircraft speeds. For example, A and F denote speeds at which a gust of velocity $\pm U_1$ would stall the wing.

The lift coefficient–incidence curve is, as we noted in connection with the flight envelope, affected by compressibility and therefore altitude so that a series of gust envelopes should be drawn for different altitudes. An additional variable in the equations for gust load factor is the wing loading w. Further gust envelopes should therefore be drawn to represent different conditions of aircraft loading.

Typical values of U_1, U_2 and U_3 are 20 m/s, 15.25 m/s and 7.5 m/s. It can be seen from the gust envelope that the maximum gust load factor occurs at the cruising speed V_C. If this value of n exceeds that for the corresponding flight envelope case, that is n_1, then the gust case will be the most critical in the cruise. Let us consider a civil, non-aerobatic aircraft for which $n_1 = 2.5$, $w = 2400\,\text{N/m}^2$ and $\partial C_L/\partial\alpha = 5.0/\text{rad}$. Taking $F = 0.715$ we have, from Eq. (14.33)

$$n = 1 + \frac{\frac{1}{2} \times 1.223\, V_C \times 5.0 \times 0.715 \times 15.25}{2400}$$

giving $n = 1 + 0.0139 V_C$, where the cruising speed V_C is expressed as an EAS. For the gust case to be critical

$$1 + 0.0139\, V_C > 2.5$$

or

$$V_C > 108\,\text{m/s}$$

Thus, for civil aircraft of this type having cruising speeds in excess of 108 m/s, the gust case is the most critical. This would, in fact, apply to most modern civil airliners.

Although the same combination of V and n in the flight and gust envelopes will produce the same total lift on an aircraft, the individual wing and tailplane loads will be different, as shown previously (see the derivation of Eq. (14.33)). This situation can be important for aircraft such as the Airbus, which has a large tailplane and a CG forward of the aerodynamic centre. In the flight envelope case the tail load is downwards whereas in the gust case it is upwards; clearly there will be a significant difference in wing load.

The transference of manoeuvre and gust loads into bending, shear and torsional loads on wings, fuselage and tailplanes has been discussed in Section 12.1. Further loads arise from aileron application, in undercarriages during landing, on engine mountings and during crash landings. Analysis and discussion of these may be found in Ref. [6].

References

1 Zbrozek, J. K., Atmospheric gusts – present state of the art and further research, *J. Roy. Aero. Soc.*, January 1965.

2 Cox, R. A., A comparative study of aircraft gust analysis procedures, *J. Roy. Aero. Soc.*, October 1970.

3 Bisplinghoff, R. L., Ashley, H. and Halfman, R. L., *Aeroelasticity*, Addison-Wesley Publishing Co. Inc., Cambridge, Mass., 1955.

4 Babister, A. W., *Aircraft Stability and Control*, Pergamon Press, London, 1961.

5 Zbrozek, J. K., *Gust Alleviation Factor*, R. and M. No. 2970, May 1953.
6 *Handbook of Aeronautics No. 1. Structural Principles and Data*, 4th edition, The Royal Aeronautical Society, 1952.

Problems

P.14.1 The aircraft shown in Fig. P. 14.1(a) weighs 135 kN and has landed such that at the instant of impact the ground reaction on each main undercarriage wheel is 200 kN and its vertical velocity is 3.5 m/s.

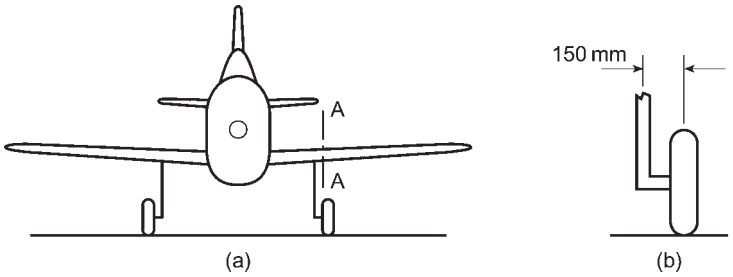

Fig. P.14.1

If each undercarriage wheel weighs 2.25 kN and is attached to an oleo strut, as shown in Fig. P.8.1(b), calculate the axial load and bending moment in the strut; the strut may be assumed to be vertical. Determine also the shortening of the strut when the vertical velocity of the aircraft is zero.

Finally, calculate the shear force and bending moment in the wing at the section AA if the wing, outboard of this section, weighs 6.6 kN and has its CG 3.05 m from AA.

Ans. 193.3 kN, 29.0 kN m (clockwise); 0.32 m; 19.5 kN, 59.6 kN m (anticlockwise).

P.14.2 Determine, for the aircraft of Example 14.2, the vertical velocity of the nose wheel when it hits the ground.

Ans. 3.1 m/s.

P.14.3 Figure P.14.3 shows the flight envelope at sea-level for an aircraft of wing span 27.5 m, average wing chord 3.05 m and total weight 196 000 N. The aerodynamic centre is 0.915 m forward of the CG and the centre of lift for the tail unit is 16.7 m aft of the CG. The pitching moment coefficient is

$$C_{M,0} = -0.0638 \text{ (nose-up positive)}$$

both $C_{M,0}$ and the position of the aerodynamic centre are specified for the complete aircraft less tail unit.

For steady cruising flight at sea-level the fuselage bending moment at the CG is 600 000 Nm. Calculate the maximum value of this bending moment for the given flight envelope. For this purpose it may be assumed that the aerodynamic loadings on the

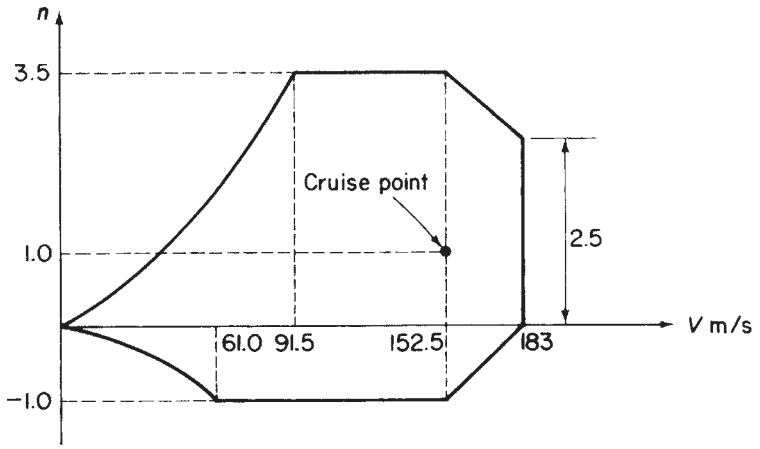

Fig. P.14.3

fuselage itself can be neglected, i.e. the only loads on the fuselage structure aft of the CG are those due to the tail lift and the inertia of the fuselage.

Ans. 1 549 500 N m at $n = 3.5$, $V = 152.5$ m/s.

P.14.4 An aircraft weighing 238 000 N has wings 88.5 m^2 in area for which $C_D = 0.0075 + 0.045C_L^2$ The extra-to-wing drag coefficient based on wing area is 0.0128 and the pitching moment coefficient for all parts excluding the tailplane about an axis through the CG is given by $C_M \cdot c = (0.427C_L - 0.061)$m. The radius from the CG to the line of action of the tail lift may be taken as constant at 12.2 m. The moment of inertia of the aircraft for pitching is 204 000 kg m^2.

During a pull-out from a dive with zero thrust at 215 m/s EAS when the flight path is at 40° to the horizontal with a radius of curvature of 1525 m, the angular velocity of pitch is checked by applying a retardation of 0.25 rad/s^2. Calculate the manoeuvre load factor both at the CG and at the tailplane CP, the forward inertia coefficient and the tail lift.

Ans. $n = 3.78$(CG), $n = 5.19$ at TP, $f = -0.370$, $P = 18\,925$ N.

P.14.5 An aircraft flies at sea level in a correctly banked turn of radius 610 m at a speed of 168 m/s. Figure P.14.5 shows the relative positions of the CG, aerodynamic centre of the complete aircraft less tailplane and the tailplane centre of pressure for the aircraft at zero lift incidence.

Calculate the tail load necessary for equilibrium in the turn. The necessary data are given in the usual notation as follows:

Weight $W = 133\,500$ N	$dC_L/d\alpha = 4.5$/rad
Wing area $S = 46.5$ m^2	$C_D = 0.01 + 0.05C_L^2$
Wing mean chord $\bar{c} = 3.0$ m	$C_{M,0} = -0.03$

Ans. 73 160 N

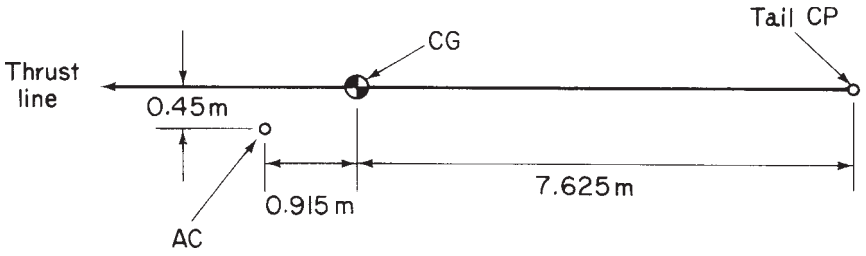

Fig. P.14.5

P.14.6 The aircraft for which the stalling speed V_S in level flight is 46.5 m/s has a maximum allowable manoeuvre load factor n_1 of 4.0. In assessing gyroscopic effects on the engine mounting the following two cases are to be considered:

(a) Pull-out at maximum permissible rate from a dive in symmetric flight, the angle of the flight path to the horizontal being limited to 60° for this aircraft.

(b) Steady, correctly banked turn at the maximum permissible rate in horizontal flight.

Find the corresponding maximum angular velocities in yaw and pitch.

Ans. (a) Pitch, 0.37 rad/s, (b) Pitch, 0.41 rad/s, Yaw, 0.103 rad/s.

P.14.7 A tail-first supersonic airliner, whose essential geometry is shown in Fig. P.14.7, flies at 610 m/s true airspeed at an altitude of 18 300 m. Assuming that thrust and drag forces act in the same straight line, calculate the tail lift in steady straight and level flight.

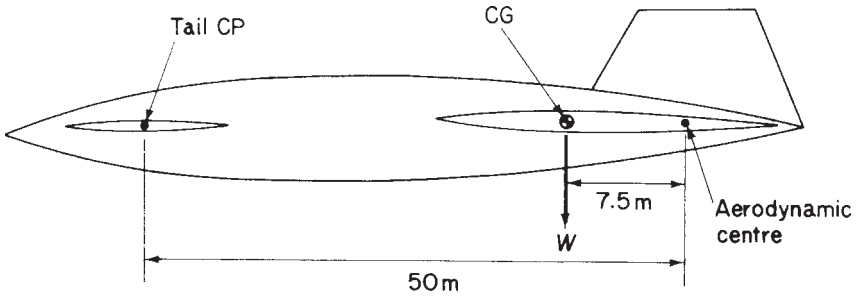

Fig. P.14.7

If, at the same altitude, the aircraft encounters a sharp-edged vertical up-gust of 18 m/s true airspeed, calculate the changes in the lift and tail load and also the resultant load factor n.

The relevant data in the usual notation are as follows:

$$\begin{aligned} \text{Wing: } S &= 280\,\text{m}^2, & \partial C_\text{L}/\partial\alpha &= 1.5 \\ \text{Tail: } S_\text{T} &= 28\,\text{m}^2, & \partial C_{\text{L,T}}/\partial\alpha &= 2.0 \\ \text{Weight } W &= 1\,600\,000\,\text{N} \\ C_{\text{M,0}} &= -0.01 \\ \text{Mean chord } \bar{c} &= 22.8\,\text{m} \end{aligned}$$

At 18 300 m

$$\rho = 0.116\,\text{kg/m}^3$$

Ans. $P = 267\,852\,\text{N}$, $\Delta P = 36\,257\,\text{N}$, $\Delta L = 271\,931\,\text{N}$, $n = 1.19$

P.14.8 An aircraft of all up weight 145 000 N has wings of area $50\,\text{m}^2$ and mean chord 2.5 m. For the whole aircraft $C_\text{D} = 0.021 + 0.041C_\text{L}^2$, for the wings $\text{d}C_\text{L}/\text{d}\alpha = 4.8$, for the tailplane of area $9.0\,\text{m}^2$, $\text{d}C_{\text{L,T}}/\text{d}\alpha = 2.2$ allowing for the effects of downwash, and the pitching moment coefficient about the aerodynamic centre (of complete aircraft less tailplane) based on wing area is $C_{\text{M,0}} = -0.032$. Geometric data are given in Fig. P.14.8.

During a steady glide with zero thrust at 250 m/s EAS in which $C_\text{L} = 0.08$, the aircraft meets a downgust of equivalent 'sharp-edged' speed 6 m/s. Calculate the tail load, the gust load factor and the forward inertia force, $\rho_0 = 1.223\,\text{kg/m}^3$.

Ans. $P = -28\,902\,\text{N}$ (down), $n = -0.64$, forward inertia force = 40 703 N.

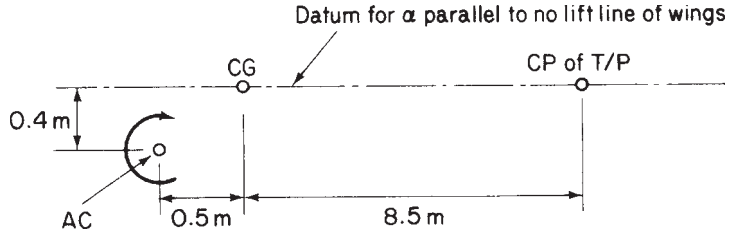

Fig. P.14.8